

# CHAPTER IV

## RESULTS AND DISCUSSION

### 4.1 The Effect of Solvent Types on the Sol-Gel Reaction

It is important to note that the NR solution in the sol-gel reaction is composed of hydrophilic part of water and hydrophobic part of NR matrix and TEOS. To prevent the phase separation between the hydrophilic and hydrophobic parts, the solvent effect on the sol-gel reaction was firstly investigated. The solvents used in this study were THF,  $\text{CHCl}_3$  and  $\text{CCl}_4$ . Their physical properties were revealed in Table 4.1. Table 4.2 shows the solvent effect on the *in situ* silica content in NR matrix. The mole ratio of TEOS to  $\text{H}_2\text{O}$  at 1:1.8 and 0.093 M *n*-hexylamine were kept constant at room temperature. It was found that the lower amount of *in situ* silica in rubbery matrix was generated when  $\text{CCl}_4$  and  $\text{CHCl}_3$  were used compared with THF. It was due to the different nature of solvent [12]. Poor water solubility and low polarity (low dielectric constant values) of  $\text{CCl}_4$  and  $\text{CHCl}_3$  was not favorable for penetration of silanol group or water during the hydrolysis and condensation reactions in sol-gel process. Therefore, THF was chosen to be a solvent that produced the high *in situ* silica content in this study.

**Table 4.1** Physical properties of solvents.

Solvents	Molecular weight <sup>a</sup>	Boiling point (°C)	Density <sup>b</sup>	Dielectric constant ( $\epsilon_r$ )	Solubility in water <sup>c</sup>
Tetrahydrofuran (THF)	72.11	66	889	7.52 (22°C)	30.0
Chloroform ( $\text{CHCl}_3$ )	119.38	61	1480	4.81 (20°C)	0.80
Carbontetrachloride ( $\text{CCl}_4$ )	153.82	77	1584	2.24 (20°C)	0.05

<sup>a</sup>  $10^{-3}$  kg/mol

<sup>b</sup> kg/m<sup>3</sup>

<sup>c</sup> kg/100 kg at 20 °C

**Table 4.2** The effect of solvent on the *in situ* silica content in NR matrix

Solvents	Catalyst	Catalyst concentration (M)	Mole ratio of TEOS:Water	Temperature	Silica content <sup>a</sup> (%)
CCl <sub>4</sub>	n-hexylamine	0.0930	1:1.8	R.T.	10 <sup>b</sup>
CHCl <sub>3</sub>	n-hexylamine	0.0930	1:1.8	R.T.	12 <sup>b</sup>
THF	n-hexylamine	0.0930	1:1.8	R.T.	38 <sup>b</sup>

<sup>a</sup> Determined by TGA

<sup>b</sup> Reaction time 14 days

#### 4.2 The Effect of Catalyst Type on Sol-Gel Reaction

As mentioned above, the sol-gel reaction system contained both the hydrophilic (water) and hydrophobic (rubber) parts. Thus, to obtain the high compatibility between the two parts, the base catalyst used were composed of hydrophobic and hydrophilic parts in the molecule. The results of sol-gel reaction using various types of catalyst (*n*-butylamine and *n*-hexylamine) are reported in Table 4.3 and Figure 4.1. The mole ratio of TEOS to H<sub>2</sub>O at 1:2.2 and the catalyst concentration of 0.093 M were kept constant at room temperature and the THF was used as solvent. The higher amount of *in situ* silica (35%) in the rubbery matrix was achieved by using *n*-hexylamine as the catalyst. It was due to the fact that the longer chain of *n*-hexylamine easily penetrated into NR matrix which containing TEOS and formed the reverse micelles like a surfactant in the TEOS-swollen NR matrix [46-47] as shown in Figure 4.2. This exhibition corresponds with the previous results of Ikeda *et al.* [15]. It was also indicated that the use of long hydrocarbon segment of primary alkyl amines resulted not only in the increase of silica content but also the acceleration of sol-gel reaction as the increasing slope of sol-gel reaction curve.

**Table 4.3** The effect of catalyst types on *in situ* silica content in NR matrix

Solvent	Mole ratio of TEOS : H <sub>2</sub> O	Catalyst	Catalyst concentration (M)	Reaction time (days)	Silica content <sup>a</sup> (%)
THF	1:2.2	<i>n</i> -butylamine	0.093	0	0
				2	10
				7	17
				14	25
				21	30
-----					
THF	1:2.2	<i>n</i> -hexylamine	0.093	0	0
				5	22
				7	23
				14	31
				21	35

<sup>a</sup> Determined by TGA

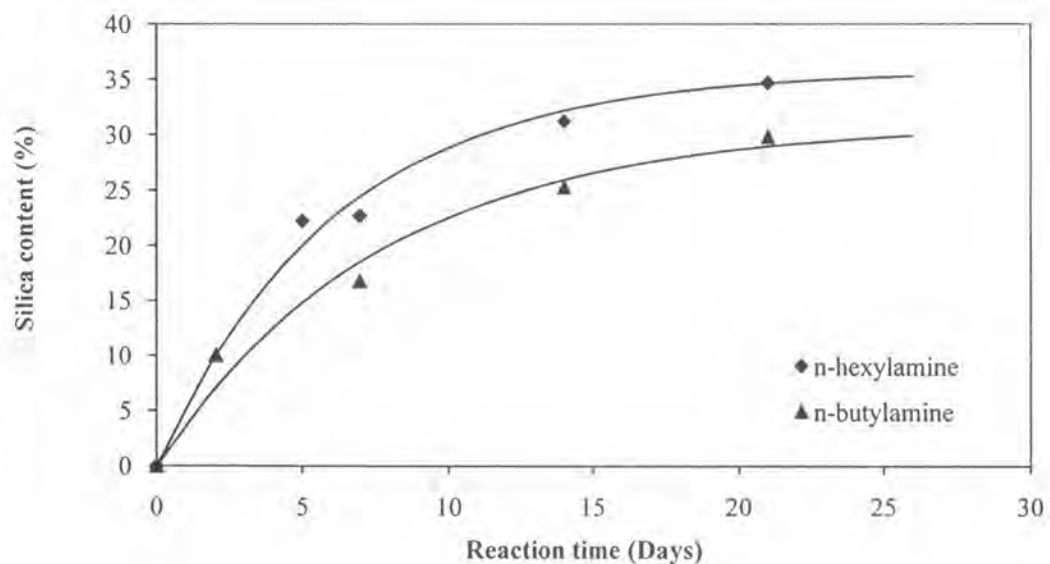


**Figure 4.1** Effect of catalyst type on the sol-gel reaction: catalyst concentration of 0.093 M and TEOS:H<sub>2</sub>O mole ratio of 1:2.2 at room temperature.

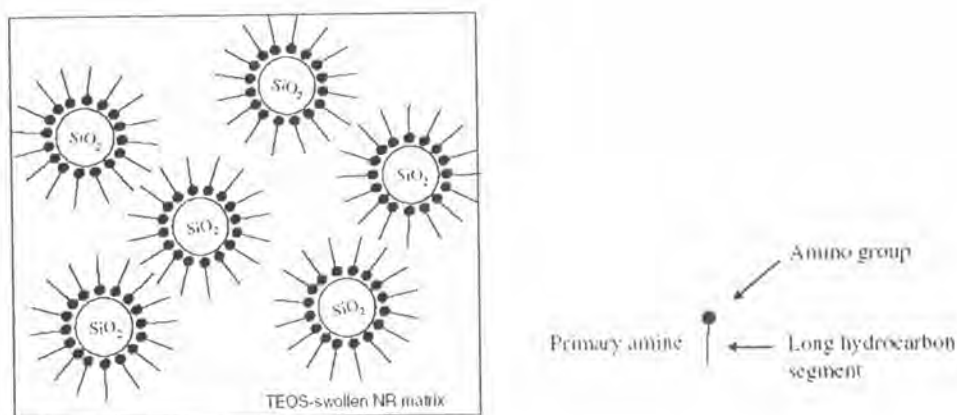


**Figure 4.2** Speculated formation of *in situ* silica in TEOS-swollen NR matrix by primary alkylamine with long hydrocarbon segment [15].

#### 4.3 The Effect of Catalyst Concentration on Sol-Gel Reaction

Table 4.3 shows the effect of catalyst concentration on *in situ* silica contents in NR matrix. The concentration of *n*-butylamine and *n*-hexylamine were varied from 0.093 M to 0.1816 M and used the mole ratio of TEOS to water 1:2.2 at the room temperature in THF. For reaction time of 14 days, the *in situ* silica content in the rubber matrix increased with increasing catalyst concentration in both types of catalyst. The relationship between the *in situ* silica content and the catalyst concentration are displayed in Figure 4.3. It presented that the slope of sol-gel reaction curve increased with increasing catalyst concentration. This result implied that the sol-gel reaction rate increased with increasing the catalyst concentration. Since more concentration of base catalyst (*n*-butylamine and *n*-hexylamine) like to accelerate water dissociation to produce more nucleophilic hydroxyl anion in a rapid first step of hydrolysis reaction. It attacked the silicon atom on TEOS as shown in Scheme 2.7 resulting in accelerate the production of hydroxyl group on the TEOS surface. The high amount of *in situ* silica in the rubbery matrix was achieved by using *n*-hexylamine. This result was corresponding with the previous work of Ikeda *et al.* [15]. They studied the effect of amine (*n*-hexylamine) on the *in situ* silica generation in NR and found that the amount of generated *in situ* silica increased with increasing *n*-hexylamine concentration. Unfortunately the sol-gel reaction in this study at the

concentration of 0.1816 M *n*-hexylamine could not be performed due to the limitation of the catalyst solubility in water, resulting in phase separation.

**Table 4.3** The effect of catalyst concentration on *in situ* silica content in NR matrix.

Solvent	Catalyst	Mole ratio of TEOS : H <sub>2</sub> O	Temperature	Catalyst concentration (M)	Silica content (%) <sup>a</sup>
				0.000	0
				0.0640	20
THF	<i>n</i> -butylamine	1:2.2	R.T.	0.0930	23
				0.1395	27
				0.1860	31
-----					
				0.000	0
				0.0640	25
THF	<i>n</i> -hexylamine	1:2.2	R.T.	0.0930	29
				0.1395	34
				0.1860	b

<sup>a</sup> Determined by TGA at reaction time 14 days

<sup>b</sup> Phase separation

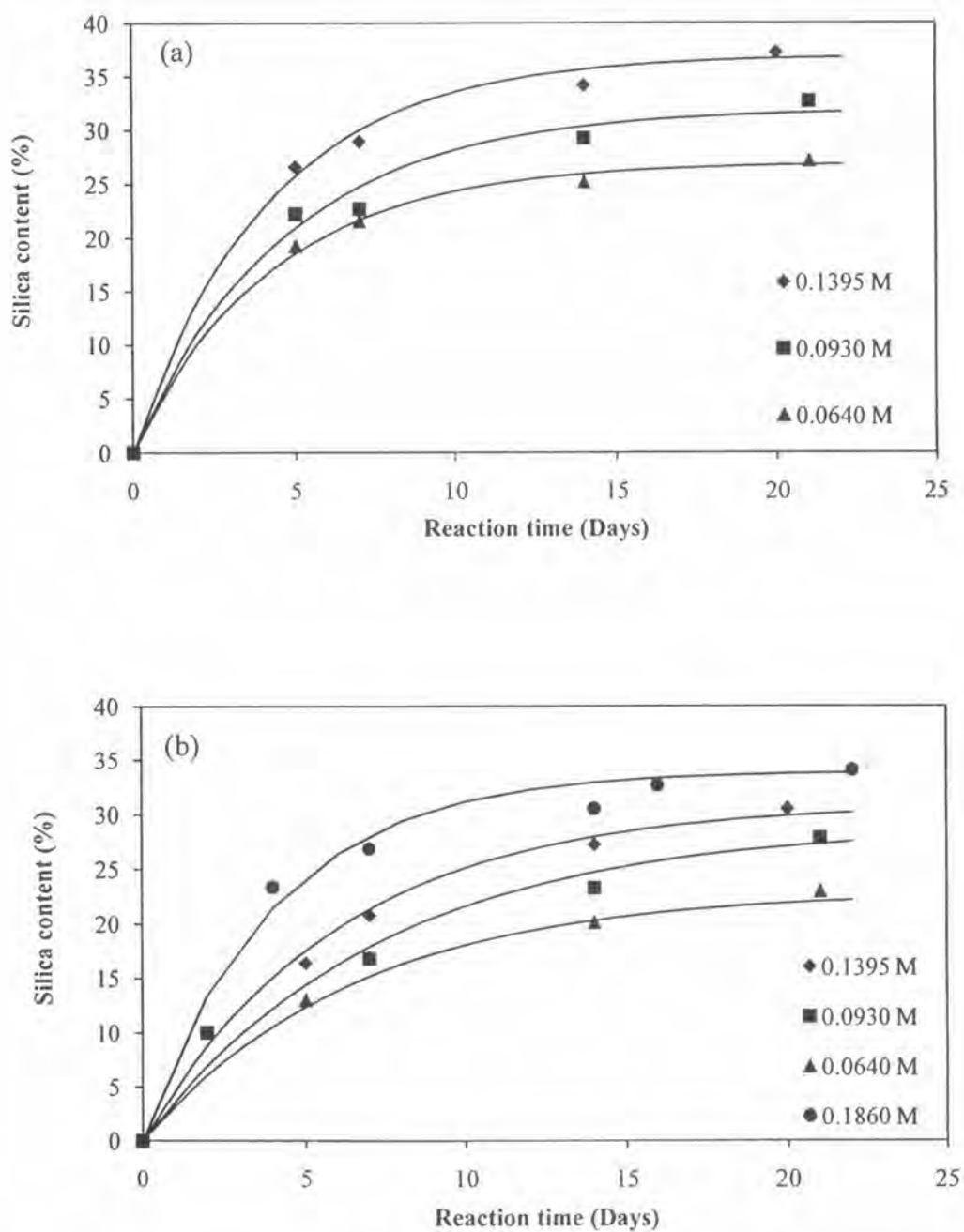


**Figure 4.3** Effect of catalyst concentration on the sol-gel reaction: TEOS:H<sub>2</sub>O mole ratio of 1:2.2 and reaction time of 14 days : (a) *n*-hexylamine (b) *n*-butylamine.

#### 4.4 The Effect of Mole Ratio of TEOS to Water on Sol-Gel Reaction

From the previous result, the most efficient sol-gel reaction condition generated in THF and *n*-hexylamine 0.1395 M was used as catalyst. The next parameter that was chosen to investigate was the mole ratio of TEOS to water. The proportion of alkoxy silane (TEOS) to water ratio was also important. Since the hydrolysis reaction of TEOS was the first stage for the sol-gel reaction. Therefore, the relationship between the silica content and reaction time at various ratios of TEOS to H<sub>2</sub>O was studied. The variation of the TEOS to the water mole ratio 1:1.8 to 1:3.0 was investigated. From Table 4.4 and Figure 4.4, the *in situ* silica contents increased with increasing mole ratio of TEOS to water since the increase in mole ratio of TEOS to water promoted the rate of hydrolysis reaction and affected to more complete hydrolysis of TEOS. After that the condensation occurred resulted in the increase of *in situ* silica content in NR matrix. This result corresponds with the previous studied of Bandyopadhyay *et al.*[12]. They studied the effect of reactants of the structure and properties of epoxidised natural rubber/ *in situ* silica nanocomposites and reported that the *in situ* silica contents increased with increasing mole ratio of TEOS to water. However this study, it indicated that the phase separation between rubbery matrix containing TEOS and H<sub>2</sub>O occurred when the ratio of TEOS to H<sub>2</sub>O was larger than 1:3 due to the solubility limitation of *n*-hexylamine in water.

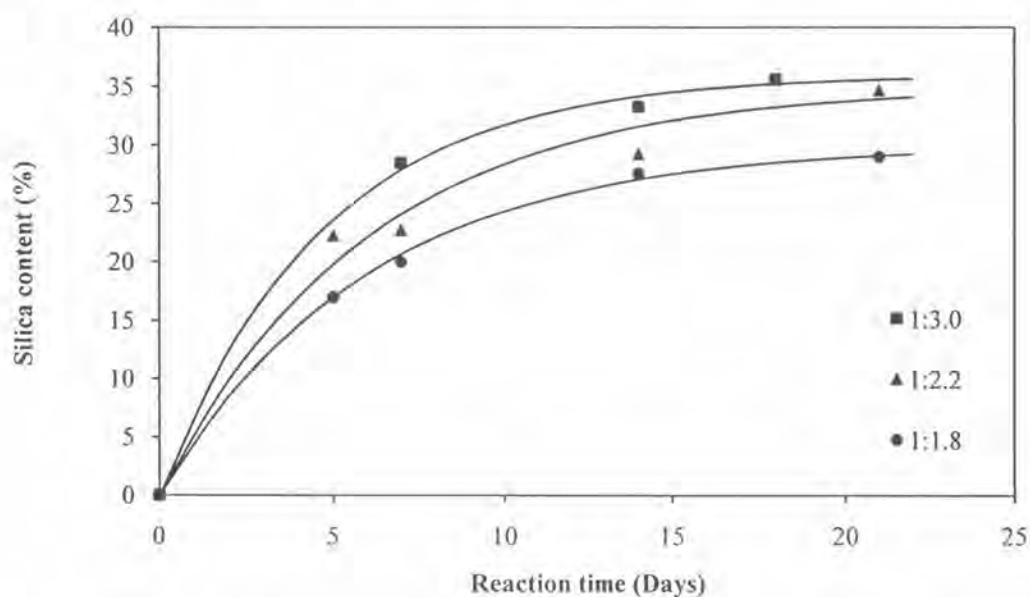


**Figure 4.4** Effect of mole ratio of TEOS:H<sub>2</sub>O on the sol-gel reaction: 0.093 M *n*-hexylamine as catalyst at room temperature.



**Table 4.4** The effect of mole ratio of TEOS to water on *in situ* silica content in NR matrix.

Solvent	Mole ratio of TEOS : H <sub>2</sub> O	Catalyst	Catalyst concentration (M)	Reaction time (Days)	Silica content <sup>a</sup> (%)
THF	1:1.8	<i>n</i> -hexylamine	0.0930	0	0
				5	17
				7	20
				14	28
				21	29
-----					
THF	1:2.2	<i>n</i> -hexylamine	0.0930	0	0
				5	22
				7	23
				14	29
				21	35
-----					
THF	1:3	<i>n</i> -hexylamine	0.0930	7	28
				14	33
				18	36

<sup>a</sup> Determined by TGA

#### 4.5 The Effect of Reaction Time and Reaction Temperature on Sol-Gel Reaction

The reaction temperature is the one of important parameters to produce *in situ* silica because the temperature can control the sol-gel reaction rate. The relationship between the *in situ* silica contents and the reaction temperatures (room temperature: R.T., 40, 45 and 50°C) at reaction time 14 days is concluded in Table 4.5. For reaction which used THF as the solvent, *n*-hexylamine 0.1395 M as catalyst and mole ratio of TEOS to water 1:2.7 at temperatures below 50°C condition, the silica contents in rubbery matrix increased with increasing reaction time approaching the constant limiting value after 14 days. As a rule, the higher the reaction temperature, the higher the yield in the *in situ* silica content. When the reaction temperature was high (50°C), the required reaction time for sol-gel reaction was shorter (7 days) than R.T., 40 and 45 °C as depicted in Figure 4.5. Accordingly, the optimum condition that produced the high silica content (41 % or 70 phr) in the NR matrix was 1:2.7 mole ratio of TEOS:H<sub>2</sub>O in THF and 0.1395 M *n*-hexylamine at 50 °C for 7 days.

**Table 4.5** The effect of reaction temperature on sol-gel reaction



<sup>a</sup> Determined by TGA at reaction time 14 days.

Solvent	Catalyst	Catalyst concentration (M)	Mole ratio of TEOS:water	Temperature (°C)	Silica content (%) <sup>a</sup>
				R.T.	37
THF	<i>n</i> -hexylamine	0.1395	1:2.7	40	41
				45	41
				50	43

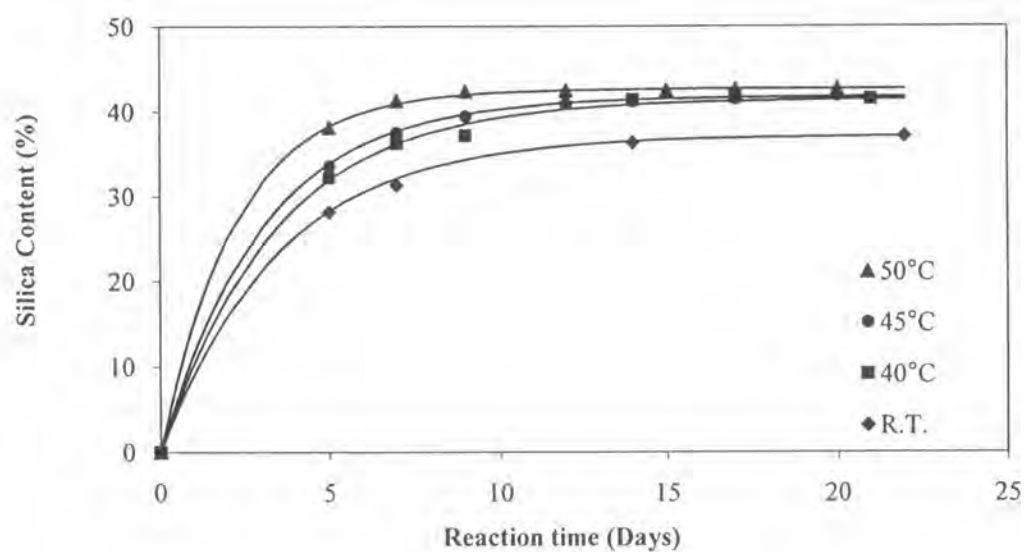
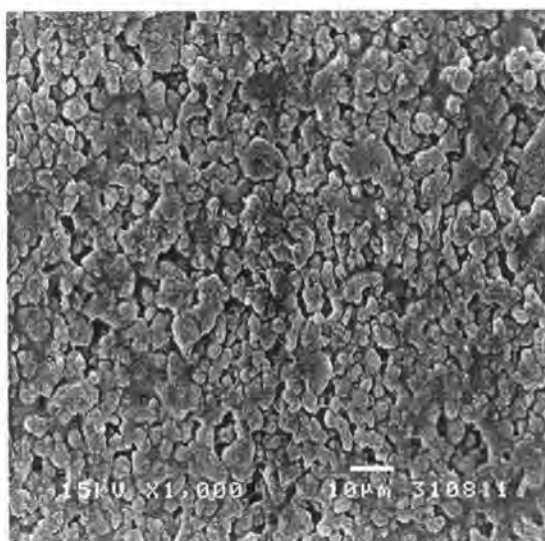


Figure 4.5 The effect of reaction time and reaction temperature on sol-gel reaction.

#### 4.6 Morphology of *In situ* Silica in NR Matrix

The SEM micrograph of *in situ* silica 41% by weight (70 phr) generated in the rubber matrix displays in Figure 4.6. The white and gray tone color represented the *in situ* silica particles and the black tone color indicated the NR matrix. The formation of filler aggregate (silica particles fused into aggregates) was clearly seen. The average diameter of aggregate size was about 2-2.5  $\mu\text{m}$ . Although, the primary particle size of the “in-situ” formed silica could not be observed by using SEM, the silica aggregates were well dispersed in rubbery matrix. The highly aggregated silica structure became significant due to the complete hydrolysis and condensation reactions. According to this result, the primary silica particles are expected to be in the nanosize due to the small size of aggregates. Therefore, it can be useful to apply “*in situ*” formed silica as reinforcing filler for composite materials.



**Figure 4.6** The morphology of *in situ* silica in natural rubber compound analyzes by SEM x 1000 magnification.

#### 4.7 Cure Characteristics Of NR Filled With Reinforcing Filler

The cure characteristics of NR vulcanizates with and without the reinforcing filler are report in Table 4.6. The Mooney viscosity ( $ML_{1+4}$ ) increased with increasing *in situ* silica contents due to the presence of rigid *in situ* silica particles with in NR matrix. It is interesting to note that the Mooney viscosity of In-30 vulcanizate was lower than that of Si-30 vulcanizate. This may be an advantage in terms of low energy consumption during rubber processing.

The curing time of *in situ* silica filled NR vulcanizates increased as the *in situ* silica contents increased, due to the surface properties of *in situ* silica. Generally, the surface of silica particles contains silanol groups, which are acidic agents and highly reactive. The silanol groups can quickly react with the curing agents, i.e., accelerator or activator which are basic and reactive, and reduces the efficiency of curing agent leading to an increase in curing time [48]. The curing time of In-30 vulcanizate was lower than that of Si-30 vulcanizate. This could be explained by differences in the surface properties of *in situ* silica from the commercial one. Indeed, using Atomic Force Microscopy (AFM), it was reported that the silanol group contents of the *in situ* silica surface was smaller than that of the commercial silica, with the decrease in the curing time of *in situ* silica filled samples being caused by the lower amount of surface silanol groups compared with that of the commercial silica [33].

However, the *in situ* silica compound remained used required the longer cure time than that of CB-30 and Ca-30 vulcanizates due to the difference in surface properties of the filler. Carbon black contains various function groups (phenolic, carboxylic, quinine and lactone groups) which capable of chemicals reacting with the rubber molecules. Calcium carbonate is basic in nature, it enhances network chain density whereas silica gives opposite results due to the containing silanol groups on the surface of the silica particles affected to delay curing process as mention above.

The addition of coupling agent (Si-69) is well established that it could be reacted with silanol group at the surface of silica particles because it is composed of two functionally active end groups, i.e., the readily hydrolysable alkoxy group ( $-C_2H_5O$ ) and the organo-functional group ( $-(CH_2)_3-S_4-(CH_2)_3$ ). The former group can react chemically with the silanol groups on silica surface to form stable siloxane linkages ( $-Si-O-Si-$ ) whereas the latter group, which is relatively non-polar, is more compatible with rubbers. This exhibit leads to decrease the filler-filler interaction and

the adsorption of accelerator on the silica surface. Therefore, the Mooney viscosity and cure time in coupling agent system are lower than the *in situ* silica filled NR vulcanizate without coupling agent [4].

**Table 4.6** Mooney viscosity and cure time of NR vulcanizates

Samples code	ML <sub>1+4</sub> (100°C)	Cure Time (min)	Curing Temperature (°C)
NR	19.7	11.3	150
In-15	20.2	11.4	150
In-30	24.8	12.3	150
In-45	27.3	14.3	150
In-65	30.6	19.3	150
Si-30	29.1	13.5	150
In-30-C	16.3	8.38	150
Si-30-C	19.3	9.33	150
CB-30	18.0	7.21	150
Ca-30	18.5	8.33	150

## 4.8 Mechanical Properties NR Vulcanizates Filled With Reinforcing Filler

### 4.8.1 The Effects of *In situ* Silica Content on Mechanical Properties

The rubber composites with different *in situ* silica content (0, 15, 30, 45 and 65 phr) were prepared by two-roll mill and the properties of *in situ* silica filled NR vulcanizates were compared. The effect of *in situ* silica content on the moduli at 50%, 100% and 300% elongation ( $M_{50}$ ,  $M_{100}$  and  $M_{300}$ ) of the *in situ* silica filled NR vulcanizates shows in Figure 4.7. All mechanical properties data of filled NR vulcanizates were reported in Table B-1 (Appendix B). The  $M_{50}$ ,  $M_{100}$  and  $M_{300}$  increased with increasing *in situ* silica contents due to the reinforcement effect of *in situ* silica. Generally, when the stress applied from an external source to the composite was transferred to the filler (which were the load-bearing element) through the filler-matrix interface [49]. Therefore, the increase of *in situ* silica content resulted in the improvement of reinforcement in NR vulcanizates.

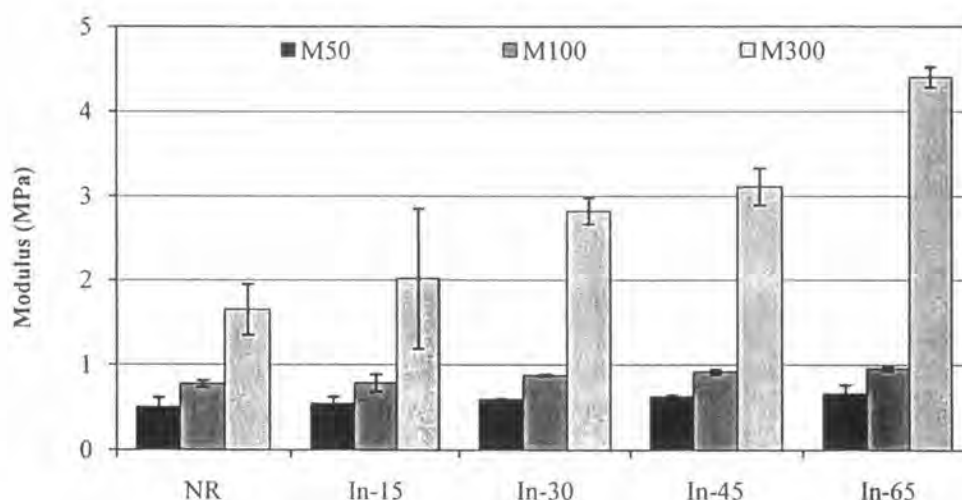


**Figure 4.7** The effect of *in situ* silica content on the modulus at 50%, 100% and 300% elongation of *in situ* silica filled NR vulcanizates.

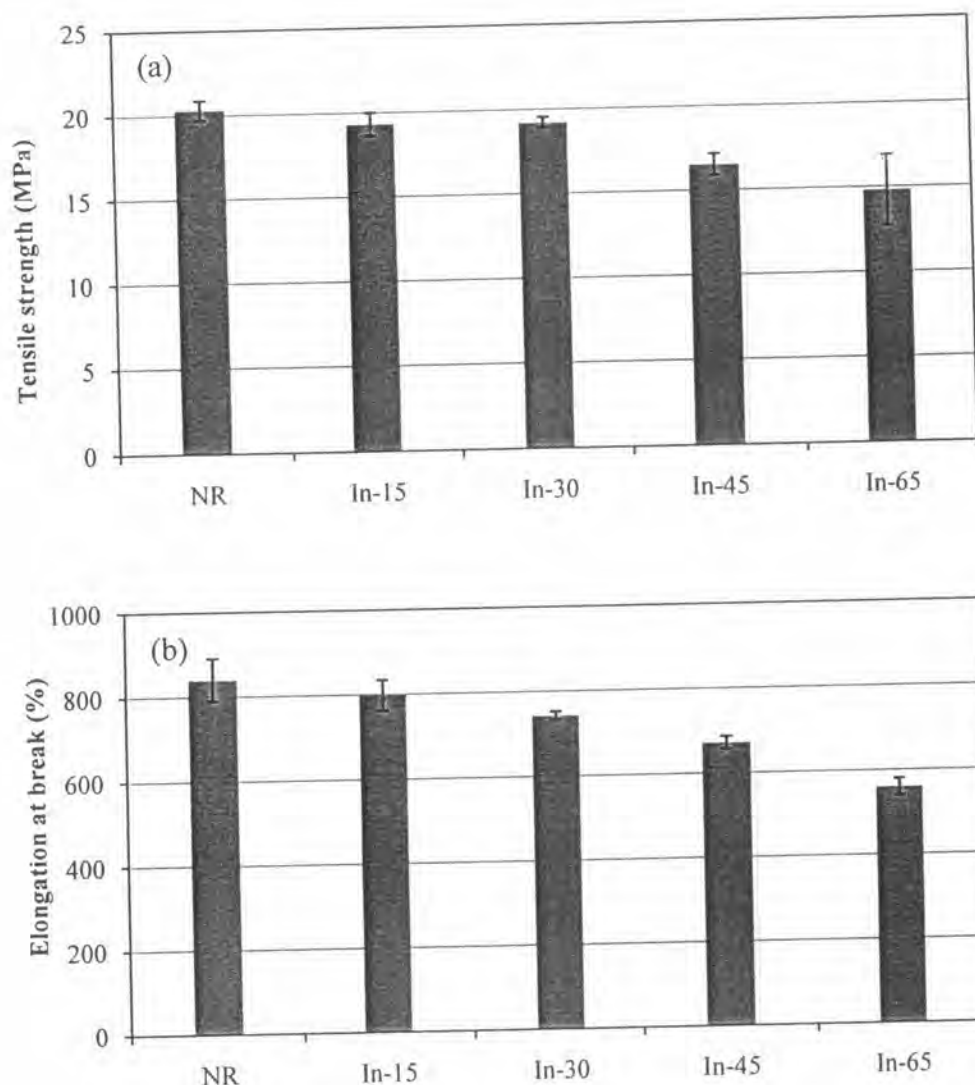


**Figure 4.8** The effect of *in situ* silica content on (a) the tensile strength and (b) the elongation at break of *in situ* silica filled NR vulcanizates.

The plots of tensile strength ( $T_B$ ) and elongation at break ( $E_B$ ) of the *in situ* silica filled NR vulcanizates versus the *in situ* silica content are illustrated in Figure 4.8. The  $T_B$  decreased with increasing *in situ* silica contents. This result may be explained by the several time of milling in the preparation of rubber compound on two-roll mill which affected to destroy the NR chain.  $E_B$  decreased with increasing *in situ* silica contents. This was expected since the network chain density of *in situ* silica filled NR vulcanizates which was determined by Flory-Rehner equation increased with increasing silica contents as reported in Table 4.7.

**Table 4.7** Network chain density of *in situ* silica filled NR vulcanizates

Sample code	Network chain densities $\times 10^4$ (mol/cm <sup>3</sup> )
NR	2.05±0.12
In-15	2.12±0.27
In-30	2.55±0.04
In-45	2.81±0.16
In-65	3.31±0.41

The hardness of the *in situ* silica filled NR vulcanizates increased continuously with increasing *in situ* silica contents as seen in Figure 4.9 (a). Generally, when silica is added into rubber at a sufficiently high loading, the distance between silica aggregates becomes close enough to induce strong interaction between aggregates giving rise to an additional network. This network should result in increasing the hardness at high silica content.

The compression set of *in situ* silica contents illustrates in Figure 4.9 (b). The compression set was found to increase continuously with increasing *in situ* silica contents. This was expected since the dilution effect. The increasing in amount of *in situ* silica would reduce the amount of rubber and thus reduced the elasticity of the NR vulcanizate. This result corresponded with the studied of Sae-oui *et al.* [50]. They reported that the increasing silica content in CR/NR blends increased the compression set. However, at the small *in situ* silica contents (15 phr), the compression set properties was improved from the NR vulcanizate since their reinforcement effect of *in situ* silica particle.

The abrasion volume loss versus the *in situ* silica content is shown in Figure 4.9 (c). The abrasion resistance of NR vulcanizate was slightly increased when the *in situ* silica contents was 15 and 30 phr due to the reinforcement effect of the filler and it decreased when silica contents was more than 45 phr. Since it was not enough the rubber matrix to hold the silica particles together lead to simply losses the rubber vulcanizate volume.



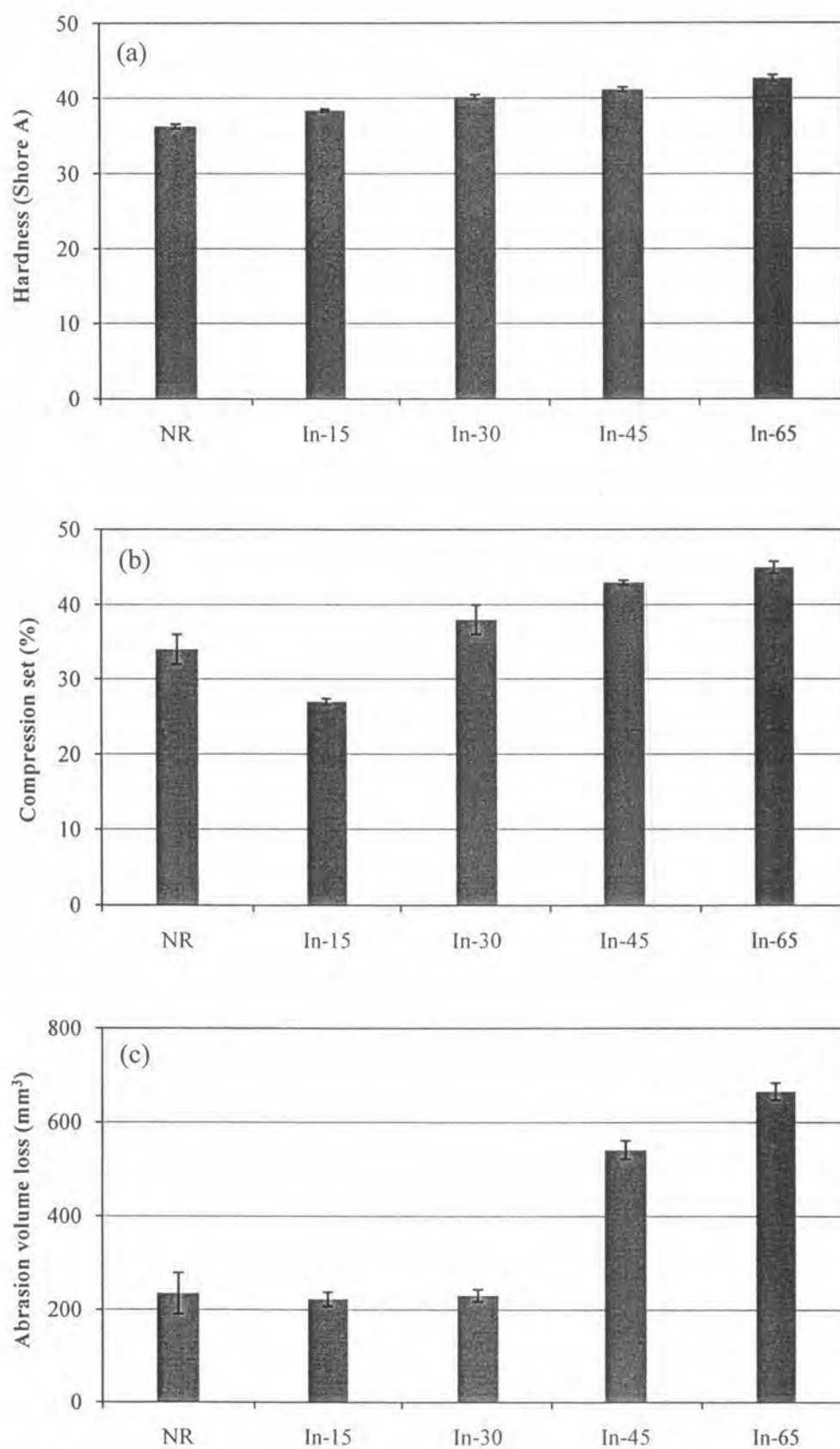


**Figure 4.9** The effect of *in situ* silica content on (a) hardness, (b) compression set and (c) abrasion resistance of *in situ* silica filled NR vulcanizates.

#### 4.8.2 Comparison of *In situ* Silica with Commercial Reinforcing Filler on Mechanical Properties

The mechanical properties of NR vulcanizates filled with reinforcing filler are shown in Figures 4.10-4.11. The  $M_{50}$ ,  $M_{100}$  and  $M_{300}$  of NR vulcanizates filled with reinforcing filler increased in following order: CB-30 > In-30 > Si-30 > Ca-30 > NR. The NR vulcanizate filled with carbon black exhibited the highest tensile properties i.e., tensile strength,  $M_{50}$ ,  $M_{100}$  and  $M_{300}$ . However it gave the lowest elongation at break since the carbon black contains the function groups (phenolic and carboxylic group) which capable of reacting with rubber molecules to form grafts during process and vulcanization and gives rise to the network chain density [51]. The NR vulcanizate filled with *in situ* silica (In-30) gave higher stress moduli than that filled with commercial silica (Si-30) because the network chain density of the In-30 vulcanizate was higher than that of the Si-30 vulcanizate as seen in Table 4.8. Additionally, the surface properties of *in situ* silica and commercial silica were different, as mentioned in cure behavior section. The NR vulcanizate filled with calcium carbonate (Ca-30) showed the lowest tensile properties compared with other reinforcing filler since the calcium carbonate used in this study was the non-reinforcing filler.

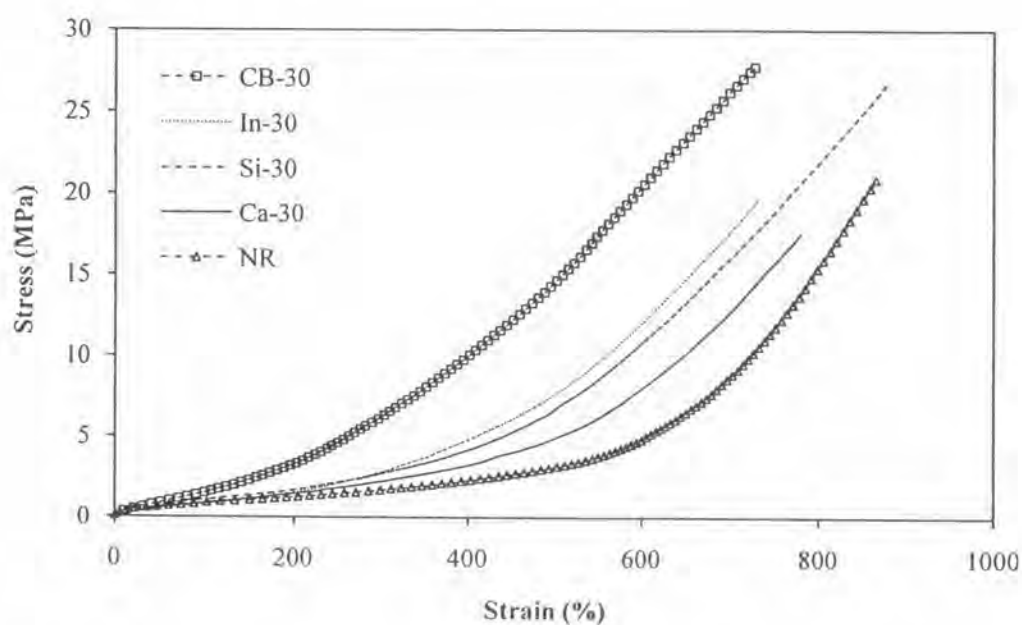
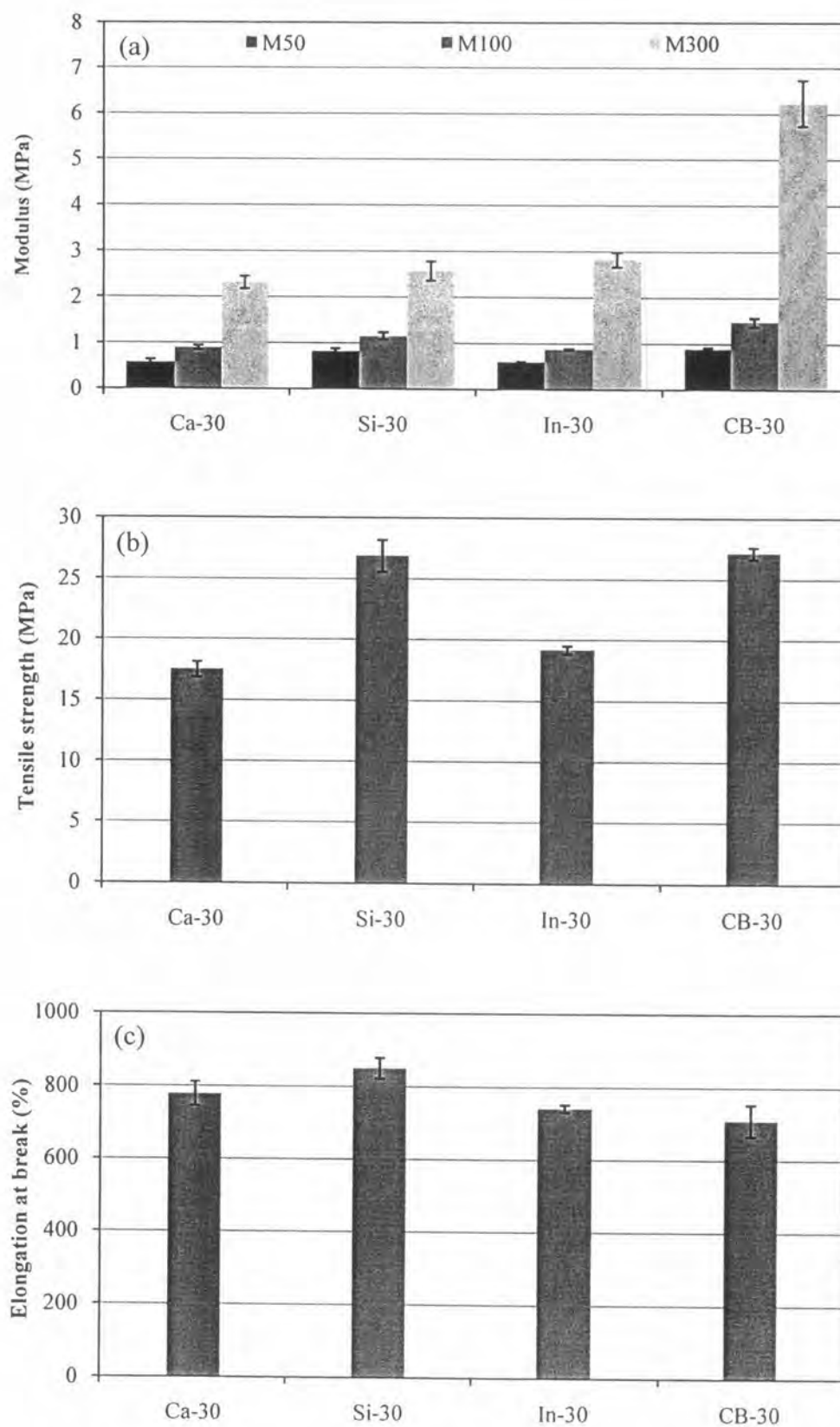


Figure 4.10 The stress-strain curve of NR vulcanizates filled with reinforcing filler.



**Figure 4.11** The tensile properties of NR vulcanizates filled with reinforcing filler (a) Modulus at 50%, 100% and 300% elongation (b) Tensile strength (c) Elongation at break.

**Table 4.8** Network chain densities of NR vulcanizates filled with reinforcing filler

Sample	Network chain densities $\times 10^4$ (mol/cm <sup>3</sup> )
In-30	2.55 $\pm$ 0.04
In-30-C	3.61 $\pm$ 0.31
Si-30	1.98 $\pm$ 0.14
Si-30-C	2.56 $\pm$ 0.16
CB-30	4.20 $\pm$ 0.59
Ca-30	2.63 $\pm$ 0.30

As illustrates in Figure 4.12 (a) the hardness of NR vulcanizates filled with reinforcing filler increased in following order: CB-30 > Si-30 > Ca-30 > In-30 vulcanizates. The hardness, compression set and abrasion resistance properties of CB-30 vulcanizate showed the highest value due to the highest network chain density. The network of silica particle gave the reinforcement effect at the small deformation but it was not stable for the large deformation [53]. Therefore, the hardness of Si-30 vulcanizate was higher than that of Ca-30 and In-30 vulcanizates, respectively. The Ca-30 vulcanizate showed higher hardness than that of In-30 vulcanizate since the aggregation of the calcium carbonate and their surface properties as mentioned in the curing behavior. This result referred that the commercial silica particles contained higher amount of filler-filler network corresponds with the Murakami *et al.* work [53]. They studied on the *in situ* silica dispersion in NR vulcanizates compared with commercial silica by AFM and reported that the silica aggregates were clearly reflected in the AFM photograph of NR vulcanizate filled with commercial silica, whereas the smoother surface was detected in *in situ* silica filled than commercial ones.

In Figure 4.12 (b), the percent compression set of Si-30 vulcanizate was the highest since the filler-filler networks was not stable for the large deformation (compression force) which caused the permanent deformation. The percent compression set of In-30 vulcanizate was lower than Ca-30 vulcanizate while the CB-30 vulcanizate gave the lowest percent compression set. As shown in the Figure 4.12 (c), the volume loss of the samples increased as follows: CB-30 < In-30 < Si-30 < Ca-30 and this result was consistent with the order of the stress-strain curve.

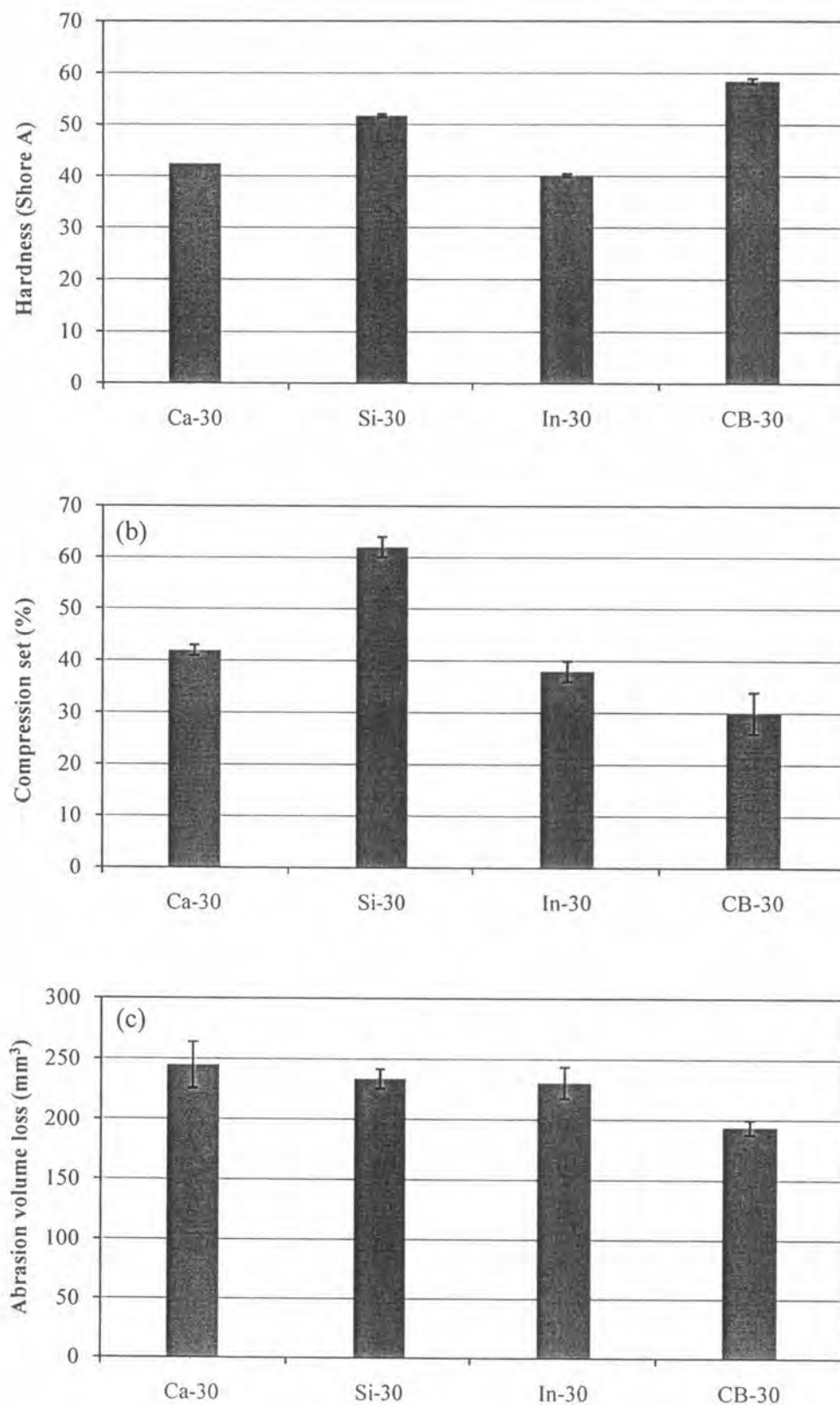


**Figure 4.12** The mechanical properties of NR vulcanizates filler with reinforcing filler (a) hardness, (b) compression set and (c) abrasion resistance.

### 4.8.3 The Effect of Coupling Agent on Mechanical Properties

The effect of silane coupling agent on tensile properties of NR vulcanizate with the reinforcing filler is illustrated in Figure 4.13. The addition of the coupling agent in to *in situ* silica filled NR vulcanizate clearly increased the tensile properties (modulus and tensile strength) and decreased the elongation at break of *in situ* silica filled NR vulcanizates as same as the effect of coupling agent on the commercial silica filled NR vulcanizates ones. It was attributed to the silane coupling reacted with the silanol groups on the surface of silica and compatible with the NR. Additionally, coupling agent also can participate in the sulfur vulcanization to form chemical linkage with NR [54]. As a consequence, silane coupling agent could act as a bridge between silica and rubber to enhance the rubber-filler interaction and increased the network chain density of the composites as reported in Table 4.8. The addition of silane coupling agent improved the hardness, compression set and abrasion resistance as shown in Figure 4.14.

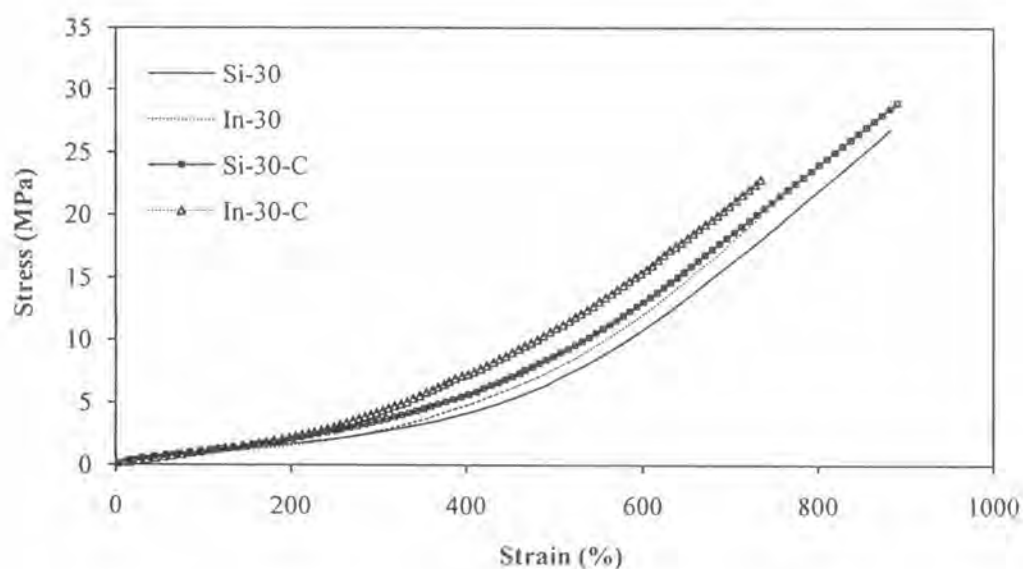


**Figure 4.13** The comparison of stress-strain curve of *in situ* silica and commercial silica filled NR vulcanizates with and without coupling agent.

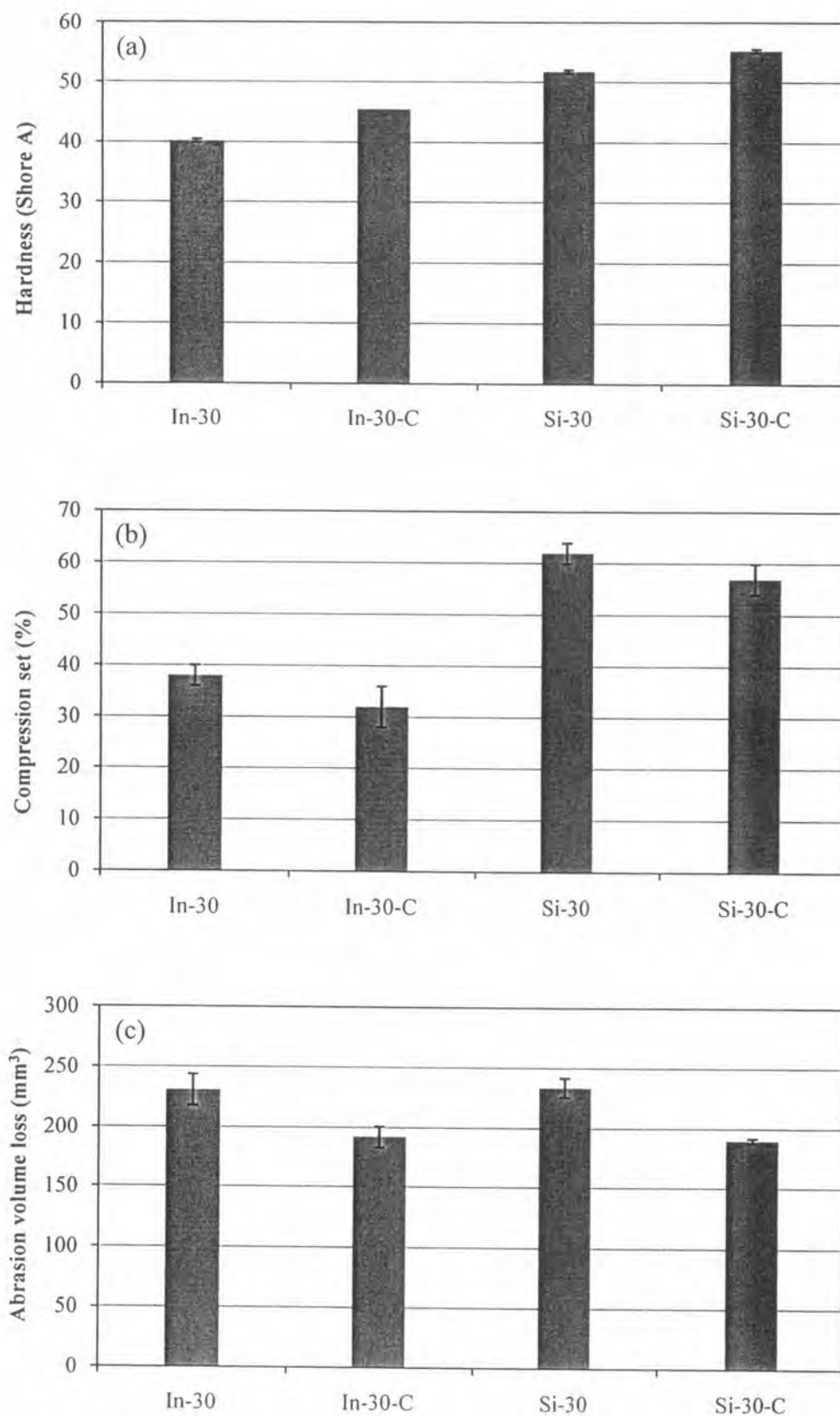


**Figure 4.14** The effect of coupling agent on (a) hardness, (b) compression set and (c) abrasion resistance of NR vulcanizates filled with silica.



#### 4.9 Morphology of Silica/NR Composites

The dispersion of *in situ* silica and commercial silica particles in NR matrix were analyzed by TEM (Figure 4.15). The black spots represent silica particles and the white area presented NR matrix. It can clearly be seen that the spherical particles of *in situ* silica were dispersed homogeneously in the NR matrix with some aggregates whilst a higher amount of aggregates of commercial silica was observed at the same filler content (30 phr). The particle size of *in situ* silica was about 60 nm and that of commercial silica was about 51 nm. These TEM observations clearly support that the surface properties of the two silica fillers are different. The well-dispersed *in situ* silica in the NR was ascribed to lower concentration of silanol groups on the surface of *in situ* silica particles compared to the Si-30 vulcanizate [19]. The lower concentrations of silanol group affected the inter-particle interaction that among *in situ* silica particles are smaller than that among the commercial silica particles in Si-30 vulcanizate.

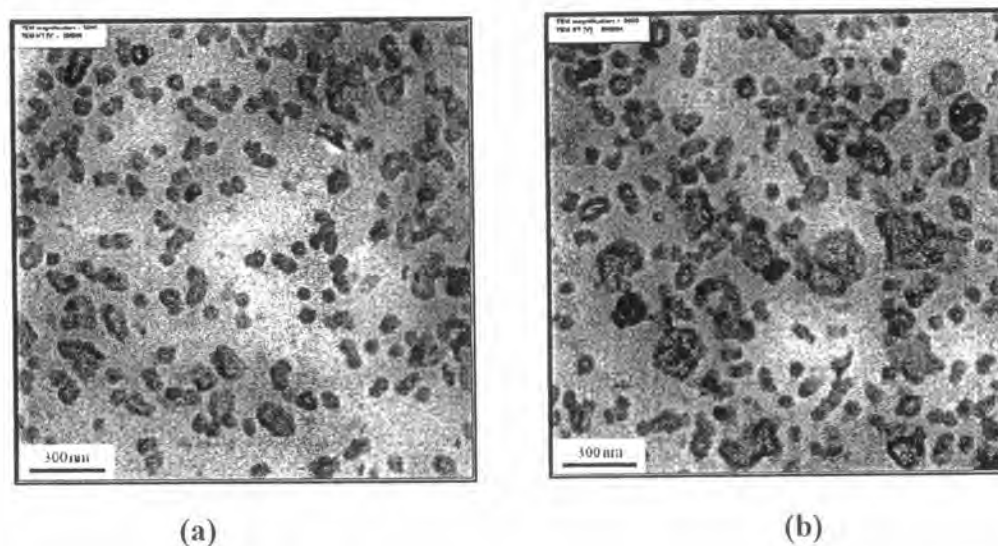


**Figure 4.15** TEM photographs of NR vulcanizates with (a) *in situ* silica 30 phr (b) commercial silica 30 phr.

#### 4.10 Dynamic Mechanical Properties of NR/Silica Composites

The storage modulus ( $E'$ ) and  $\tan \delta$  of NR vulcanizates with and without reinforcing filler show temperature-dependent dynamic behaviors with three distinct regions, e.g. glassy, transition and rubbery in Figure 4.16. The  $E'$  values in the glassy region (approximately  $-100\text{ }^{\circ}\text{C}$  to  $-70\text{ }^{\circ}\text{C}$ ) of the vulcanizate decreased in the following order: Si-30 > In-30 > NR. For the transition region, a large abrupt change in  $E'$  values took place due to the mobility gain of rubber chain segments from the glassy state to the rubbery state. Finally, a rubbery modulus was observed, but the  $E'$  value at  $25\text{ }^{\circ}\text{C}$  was still in the order Si-30 > In-30 > NR, which likely indicates that the interaction between silica filler and rubber was high in case of Si-30 vulcanizate, resulting in difficulty for movement of the rubber chain segments. In addition, for the Si-30 vulcanizate, the larger silica particle aggregates, forming a pseudo-network structure, resulted in the higher  $E'$  at  $25\text{ }^{\circ}\text{C}$  compared with that of the In-30 vulcanizate, an explanation which is consistent with the TEM observations.

The presence of reinforcing filler in the NR matrix was also found to lower and broaden the  $\tan \delta$  peak compared with that for the NR vulcanizate. The  $\tan \delta$  peaks for both filled samples were also shifted to the higher temperature region compared to NR vulcanizate as reported in Table 4.9. In general, the increasing network chain density and reinforcing filler amount make the  $\tan \delta$  peak broad and low and shifts it to a higher temperature region [5]. However, the network chain density of Si-30 vulcanizate was smaller than that of the In-30 vulcanizate, implying that the larger aggregates of commercial silica in the NR matrix restricted the motion of rubber molecules resulting in the broader  $\tan \delta$  peak compared to that of the *in situ* silica filled sample.

**Table 4.9** Dynamic mechanical properties of NR vulcanizates

	NR	In-30	Si-30
$\tan \delta$ peak position ( $^{\circ}\text{C}$ )	-57.1	-50.1	-53.3
$\tan \delta$ peak height	1.37	1.11	1.17

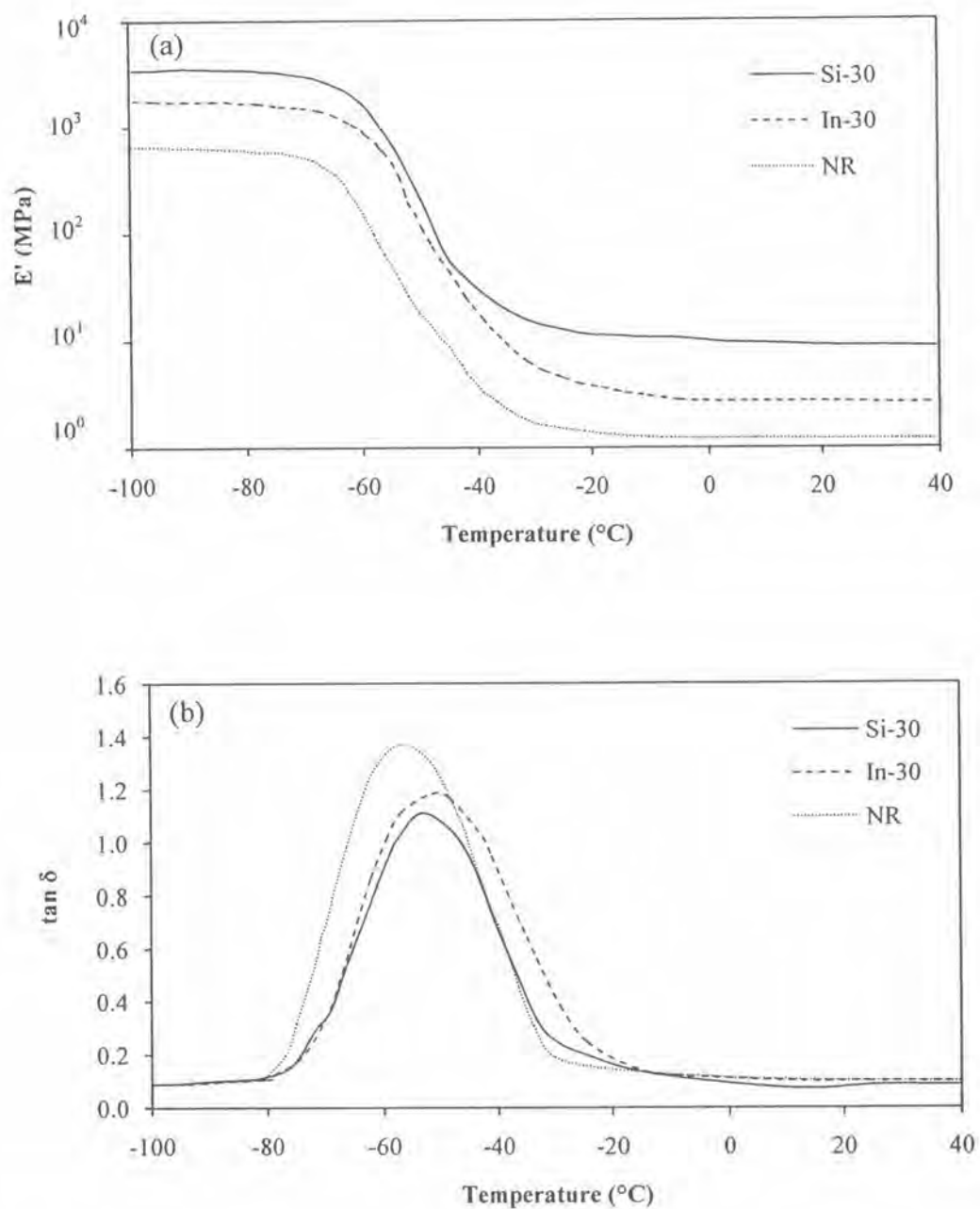


**Figure 4.16** Dynamic mechanical property analysis of NR, In-30 and Si-30 vulcanizates as described by (a) the storage modulus ( $E'$ ) and (b)  $\tan \delta$ .

#### 4.11 Thermal Properties of NR/Silica Composites

The thermal degradation characteristics of NR vulcanizates with and without the reinforcing filler are presented in Figure 4.17 and Table 4.10. From the thermogravimetric analysis (Figure 4.17), the first stage degradation of all samples started around 250 °C, and was completed at 450 °C, due to the thermal decomposition of NR. The second mass loss peak, approximately 450 °C to 570 °C was associated with the thermal decomposition of carbonaceous residues from the rubber [55]. The residual weights of silica were approximately 30 phr for both In-30 and Si-30 vulcanizates.

When compared thermal stability of NR vulcanizate with In-30 and Si-30, the thermograph of NR vulcanizate showed the delayed decomposition process than that of filled NR since the heat content of silica are higher than that of NR. The diffusion of decomposition products from the bulk polymer to gas phase is therefore slowed down. Another reason for the improvement in ageing resistance of the composites is that silica will migrate to the surface of the composites at elevated temperatures because of its relatively low surface potential energy. This migration results in the formation of a silica/NR char, which acts as a heating barrier to protect the NR inside [56]. Similar result was found in Gilman *et al.*, [57] and Vyazovkin *et al.*'s [58] work, where a clay/polymer char greatly enhances the thermal resistance of the host polymers.

The activation energy for decomposition ( $E_d$ ) of all samples was determined by the integral method of Horowitz and Metzger using equations (4.1) and (4.2) below [59], whilst  $E_d$  was calculated from the slope of the straight line of the plot  $\ln[\ln(1-\alpha)^{-1}]$  versus  $\theta$ .

$$\ln[\ln(1-\alpha)^{-1}] = E_d \theta / RT_{\max}^2 \quad (4.1)$$

$$\alpha = (C_i - C) / (C_i - C_f) \quad (4.2)$$

where  $\alpha$  is the decomposed fraction,  $C$  is the weight at the temperature chosen,  $C_i$  is the weight at initial temperature, and  $C_f$  is the weight at final temperature,  $R$  is the universal gas constant and  $\theta$  is given by  $T - T_{\max}$ .

The initial decomposition temperature ( $T_{id}$ ), the temperature of maximum weight loss rate ( $T_{\max}$ ) and the activation energy for decomposition ( $E_d$ ) of all samples were in the following order: NR < Si-30 < In-30 (Table 4.10). According to these

results, the thermal stability of the In-30 vulcanizate was improved by the presence of the *in situ* silica as reinforcing filler, and supports that the thermal stability of the In-30 vulcanizate was improved resulting in the delayed decomposition process. The higher thermal stability of the In-30 than that of the Si-30 vulcanizate may be due to the higher network chain density of the former compared to the latter. A similar result, where the addition of a coupling agent into the Si/SBR composite gave either an increased network chain density or an increased thermal stability, has been reported before [60].

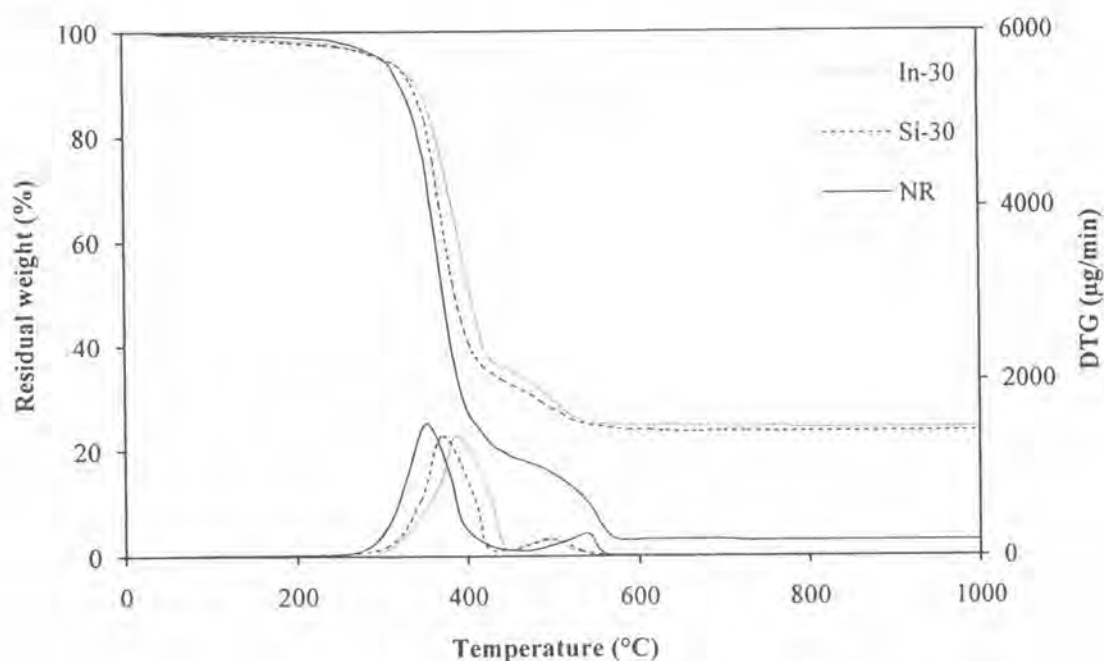


**Figure 4.17** Thermogravimetric analysis of NR, In-30 and Si-30 vulcanizates.

**Table 4.10** Thermal stability parameters of the silica/rubber composites by using Horowitz–Metzger method

Sample	$T_{id}^a$ (°C)	$T_{max}^b$ (°C)	$E_t^c$ (KJ/mol)
NR	284	351	24
Si-30	289	369	27
In-30	306	387	33

<sup>a</sup> Initial Decomposition Temperature

<sup>b</sup> Temperature of maximum rate of weight loss

<sup>c</sup> Activation energy for decomposition (Horowitz and Metzger)